LiDAR-based End-to-end Temporal Perception for Vehicle-Infrastructure Cooperation

Zhenwei Yang[1,2,†],Jilei Mao[†],Wenxian Yang[2],Yibo Ai[1],Yu Kong[4],Haibao Yu[2,3,*],Weidong Zhang[1,*]

arXiv:2411.14927v1 [cs.CV] 22 Nov 2024

***Abstract*—Temporal perception, the ability to detect and track objects over time, is critical in autonomous driving for maintaining a comprehensive understanding of dynamic environments. However, this task is hindered by significant challenges, including incomplete perception caused by occluded objects and observational blind spots, which are common in single-vehicle perception systems. To address these issues, we introduce LET-VIC, a LiDAR-based End-to-End Tracking framework for Vehicle-Infrastructure Cooperation (VIC). LET-VIC leverages Vehicle-to-Everything (V2X) communication to enhance temporal perception by fusing spatial and temporal data from both vehicle and infrastructure sensors. First, it spatially integrates Bird's Eye View (BEV) features from vehicle-side and infrastructure-side LiDAR data, creating a comprehensive view that mitigates occlusions and compensates for blind spots. Second, LET-VIC incorporates temporal context across frames, allowing the model to leverage historical data for enhanced tracking stability and accuracy. To further improve robustness, LET-VIC includes a Calibration Error Compensation (CEC) module to address sensor misalignments and ensure precise feature alignment. Experiments on the V2X-Seq-SPD dataset demonstrate that LET-VIC significantly outperforms baseline models, achieving at least a 13.7% improvement in mAP and a 13.1% improvement in AMOTA without considering communication delays. This work offers a practical solution and a new research direction for advancing temporal perception in autonomous driving through vehicle-infrastructure cooperation.**

***Index Terms*—Vehicle-Infrastructure Cooperative, End-to-End, V2X Communication, BEV Feature Fusion, Attention Mechanisms, Sensor Calibration Error Compensation, Temporal Perception.**

I. Introduction

Temporal perception, which encompasses both detection and tracking, is crucial for advanced autonomous driving. It enables Connected and Autonomous Vehicles (CAVs) to continuously identify and characterize objects while monitoring their dynamic changes over time, providing a detailed understanding of the dynamic environment. However, single-vehicle temporal perception systems face significant challenges, particularly in complex urban settings where occlusions and blind spots can limit the field of view. These limitations hinder the ability of CAVs to obtain a complete and reliable understanding of their surroundings.

[†]These authors contributed equally to this work.

[*]is the corresponding author. Contact: wdzhang@ustb.edu.cn; zwdpaper@163.com; yuhaibao94@gmail.com

[1]National Center for Materials Service Safety (NCMS), University of Science and Technology Beijing, Beijing 100083, China.

[2]Institute for AI Industry Research (AIR), Tsinghua University, Beijing 100083, China.

[3]The University of Hong Kong, Hong Kong 999077, China.

[4]Chengfang Financial Information Technology Services CO.LTD, Beijing 100031, China

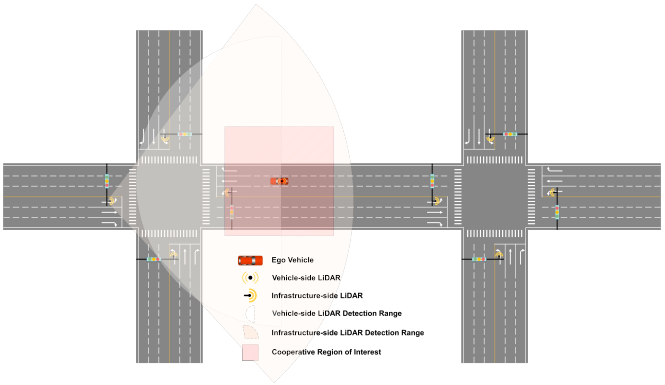

Fig. 1. **Vehicle-Infrastructure Cooperative Diagram.** The red car represents the Ego Vehicle. The vehicle-side LiDAR covers a semicircular area in front of the Ego Vehicle, while the infrastructure-side LiDAR has a fan-shaped coverage area. Through vehicle-infrastructure cooperation, the infrastructure can provide additional perception information to the vehicle.

Vehicle-Infrastructure Cooperation (VIC), enabled by advancements in Cooperative Intelligent Transportation Systems (C-ITS) and Vehicle-to-Everything (V2X) communication [1]–[3], offers a solution to the limitations of vehicle-only perception. Through V2X, data can be exchanged seamlessly between CAVs and infrastructure, allowing the integration of infrastructure-based perception information. This cooperation enhances situational awareness and fills the gaps caused by occlusions or restricted views on the vehicle side. In particular, VIC strengthens temporal perception by providing a more holistic, continuous view of the surroundings, as illustrated in Fig. 1 and Fig. 2. By combining data from both vehicle and infrastructure sensors, VIC offers more accurate and robust temporal perception compared to standalone vehicle sensors.

Despite the advantages of VIC, current VIC methods are limited in their use of temporal information. Existing approaches typically leverage temporal context only during the tracking stage, treating detection as an isolated task for each individual frame. This frame-by-frame detection fails to fully exploit the sequential information across frames, which could otherwise improve detection accuracy. Moreover, most VIC approaches focus on spatial data fusion, integrating multi-view data from vehicle-side and infrastructure-side sensors at a single moment, without extending this fusion to encompass temporal information. Consequently, these approaches are limited by their reliance on instantaneous data, missing out on the benefits of historical context for more informed decision-making.

An end-to-end approach to temporal perception, which utilizes sequential data across frames for both detection and

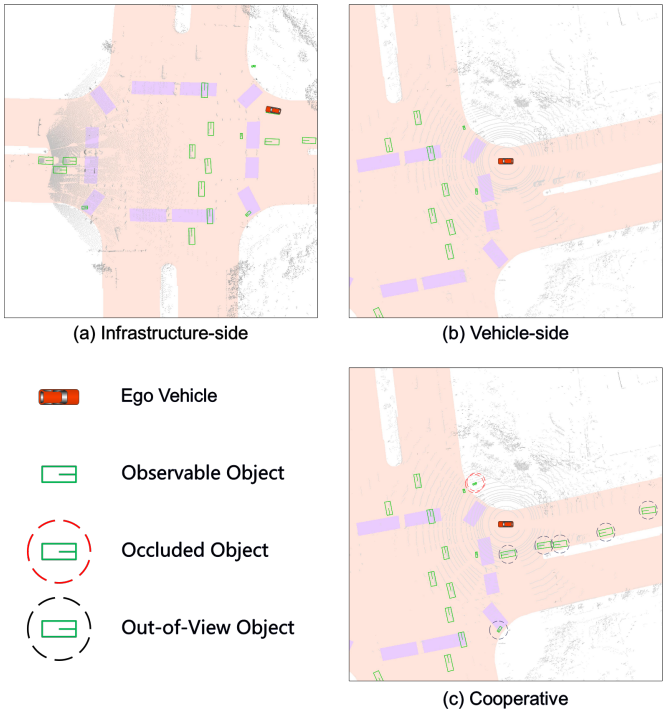

Fig. 2. **Vehicle-Infrastructure Cooperative Perception.** (a) illustrates perception using only infrastructure-side LiDAR, (b) illustrates perception using only vehicle-side LiDAR, and (c) shows the cooperative perception results combining (a) and (b). The red car represents the Ego Vehicle, green boxes indicate detected objects with their orientations, targets within the red dashed circles are those occluded from the vehicle's view, and targets within the black dashed circles are outside the vehicle's perception range.

tracking, offers a promising alternative to current VIC methods [4]–[8]. This paradigm enables a coherent understanding of object dynamics, resulting in a more robust perception system. When implemented with LiDAR technology, end-to-end temporal perception becomes even more effective. Compared to traditional camera-based systems, LiDAR provides precise distance measurements and maintains reliable performance in adverse weather and low-light conditions, making it an ideal foundation for advanced temporal perception. While LiDAR-based end-to-end temporal perception has shown strong potential in vehicle-only systems, extending this approach to a VIC-based framework that fully leverages both spatial and temporal contexts remains underdeveloped. Developing such a framework could significantly enhance safety and reliability in autonomous driving applications.

In this study, we propose LET-VIC, the first LiDAR-based End-to-end Tracking framework for VIC, which designed to address major perception challenges in autonomous driving, including limited perception range and occlusion. LET-VIC fully utilizes LiDAR point clouds from both vehicle-side and infrastructure-side sensors, incorporating temporal data to greatly enhance object detection and tracking in complex traffic environments. The framework features an advanced feature fusion strategy that uses a VIC cross-attention mechanism to seamlessly integrate Bird's Eye View (BEV) features from the infrastructure-side into the vehicle-side BEV representation. Furthermore, We employ a Calibration Error Compensation (CEC) module to compensate for calibration errors between vehicle-side and infrastructure-side sensors, delivering precise and robust 3D object perception. Rigorous testing on the V2X-Seq-SPD dataset [9], which captures challenging real-world driving scenarios, demonstrates that LET-VIC consistently outperforms existing cooperative tracking methods.

The contributions are summarized as follows:

- We introduce LET-VIC, a LiDAR-based End-to-end Tracking framework for VIC that leverages a novel VIC cross-attention mechanism to fuse BEV features from both vehicle and infrastructure side sensors, providing a unified solution for 3D object perception in complex traffic scenarios.
- We propose a self-supervised method to optimize spatial error correction during coordinate transformation. By learning offsets Δx and Δy within BEV queries, this method corrects misalignments caused by calibration errors, enhancing robustness against coordinate inaccuracies.
- LET-VIC consistently outperforms existing cooperative temporal perception methods on the V2X-Seq-SPD dataset [9]. Our experimental design also included evaluations under various delay conditions ranging from 0 ms to 300 ms, demonstrating LET-VIC's strong stability and adaptability, even though it was not explicitly optimized for delay handling.

The remainder of this paper is organized as follows. Section II reviews the related works relevant to this study. In Section III, we present LET-VIC, our proposed LiDAR-based end-to-end framework for VIC tracking. Section IV details the experimental results and analysis. Finally, Section V concludes the paper.

II. Related Works

A. Cooperative Perception

With advancements in Vehicle-to-Everything (V2X) communication technologies [10]–[13], cooperative perception in autonomous driving enhances perception capabilities through data sharing and fusion across multiple agents. This approach addresses challenges such as occlusion, long-distance perception, and sensor failures that single-vehicle perception may struggle with. Cooperative perception research primarily focuses on two types: Vehicle-to-Vehicle (V2V) and Vehicle-to-Infrastructure (V2I) cooperation.

In V2V cooperation, several methodologies have been explored. Early Fusion techniques, as seen in Cooper [14] and DiscoNet [15], integrate raw sensor data from multiple vehicles, improving detection accuracy and extending perception range. Feature Fusion approaches, such as OPV2V [16], F-Cooper [17], V2VNet [18], and COOPERNAUT [19], combine intermediate-level features from multiple vehicles for enhanced perception. Notably, How2comm [20] focuses on transmitting BEV features extracted from point clouds to enhance cooperative 3D object detection.

In contrast, V2I cooperation has been explored through models such as V2X-ViT [21], FFNet [22], CTCE [23] and V2X-Graph [24], which adopt a middle-fusion approach to integrate data from both vehicles and infrastructure. These

models account for challenges like latency and calibration errors, primarily focusing on object detection tasks. While V2V cooperation benefits from richer shared data among vehicles, V2I is especially effective in scenarios where infrastructure sensors complement vehicle perception, providing broader environmental awareness.

These diverse approaches underscore significant efforts to leverage collective sensing capabilities. These capabilities help overcome the inherent limitations of individual vehicle sensors, ultimately enhancing the reliability and safety of autonomous driving systems. While many studies focus on specific perception tasks, integrating cooperative strategies into broader end-to-end systems remains a promising direction for future research, offering the potential for more comprehensive system performance in complex driving environments.

B. End-to-End Temporal Perception

The paradigm of End-to-End Temporal Perception has redefined sequential object perception by shifting from traditional tracking-by-detection to a more integrated approach. This approach combines object detection and tracking within a unified model. Models such as MotionTrack [4], TrackFormer [5], MOTR [6], CenterTrack [7], and CenterPoint [8] exemplify this shift, with each model contributing to multi-object temporal perception through different methods, such as sensor fusion, transformer-based architectures, and point tracking.

MotionTrack [4] introduces a transformer-based end-to-end temporal perception algorithm utilizing LiDAR-camera fusion, setting a new benchmark for tracking multiple object classes with multimodal sensor inputs. TrackFormer [5] and MOTR [6] reformulate temporal perception as a set prediction problem, leveraging transformer architectures to maintain track identity and spatiotemporal trajectories without requiring separate motion or appearance modeling. CenterTrack [7] simplifies the process by performing detection and tracking simultaneously, significantly improving temporal perception efficiency and accuracy. CenterPoint [8], a LiDAR-based 3D object detection and tracking framework, introduces an anchor-free approach that directly predicts object center points and regresses their attributes.

While end-to-end temporal perception offers substantial improvements in efficiency and accuracy, these existing methods generally lack LiDAR-based multi-view information fusion, which can limit their perception capabilities in complex environments. To address this gap, we propose a novel LiDAR-based end-to-end temporal perception framework for VIC that leverages multi-view fusion between vehicle-side and infrastructure-side sensors. This framework enhances perception by integrating complementary spatial and temporal information, enabling more accurate and robust temporal perception, demonstrating a marked advancement in the domain of cooperative temporal perception.

C. BEV-based Perception

BEV-based perception has emerged as a powerful method for enhancing object detection and tracking in autonomous driving. LSS [25] pioneered the use of depth estimation to project image features into BEV space, effectively addressing the challenge of fusing multi-view image data. BEVDet4d [26] further optimized this process, while BEVDepth [27] and BEVStereo [28] improved the precision of image-to-BEV feature projection. Methods like Simple-BEV [29], Fast-BEV [30], and MatrixVT [31] made BEV feature generation more efficient, while BEVFormer [32] introduced spatial cross-attention to fuse features from different camera views in BEV space. These advancements laid the foundation for more sophisticated end-to-end autonomous driving systems [33], [34]. Additionally, recent works such as Is-Fusion [35], BEV-Fusion [36], and FusionFormer [37] have focused on multi-modal data integration, combining image and LiDAR data for more accurate perception. BEV-based perception offers significant advantages for autonomous driving by enabling accurate, unified spatial representations from multi-view and multimodal data. We adopt BEV-based perception as it allows our system to integrate multi-sensor inputs seamlessly and accurately, supporting more reliable and robust performance in dynamic driving environments.

III. Method

This section describes the LET-VIC method utilized in our proposed LiDAR-based end-to-end tracking framework for VIC. At the core of LET-VIC is the VIC Cross-Attention mechanism, which dynamically integrates LiDAR features from both vehicle-side and infrastructure-side perspectives, with a focus on each point within the ego vehicle's surrounding area. As illustrated in Fig. 3, LET-VIC leverages PointPillars [38] for feature extraction from both vehicle and infrastructure LiDAR data. The features are then fused using the VIC Cross-Attention module to enhance feature integration on the vehicle side, followed by detection and tracking using the MOTR approach [6]. Additionally, the framework addresses the significant impact of sensor calibration errors on detection and tracking accuracy through an online sensor calibration compensation module. We begin by defining the VIC temporal perception problem and providing relevant background information. Following this, we present our approach to generating BEV features and detail the methodology for effectively fusing multi-view data. We then address the significant challenge of sensor calibration errors and propose a compensation mechanism to mitigate their impact. Subsequently, we present our end-to-end temporal perception strategy. Finally, we discuss the evaluation metrics employed to assess the overall effectiveness of LET-VIC.

A. Task Description

VIC Temporal Perception encompasses the dual objectives of detecting and tracking objects using sequential point cloud data collected from both vehicle and infrastructure sensors. This collaborative approach enhances the overall perception of the environment, allowing for more accurate identification and monitoring of objects within the vicinity of the ego vehicle [9]. The study focuses specifically on point cloud data, which contains critical depth information obtained from

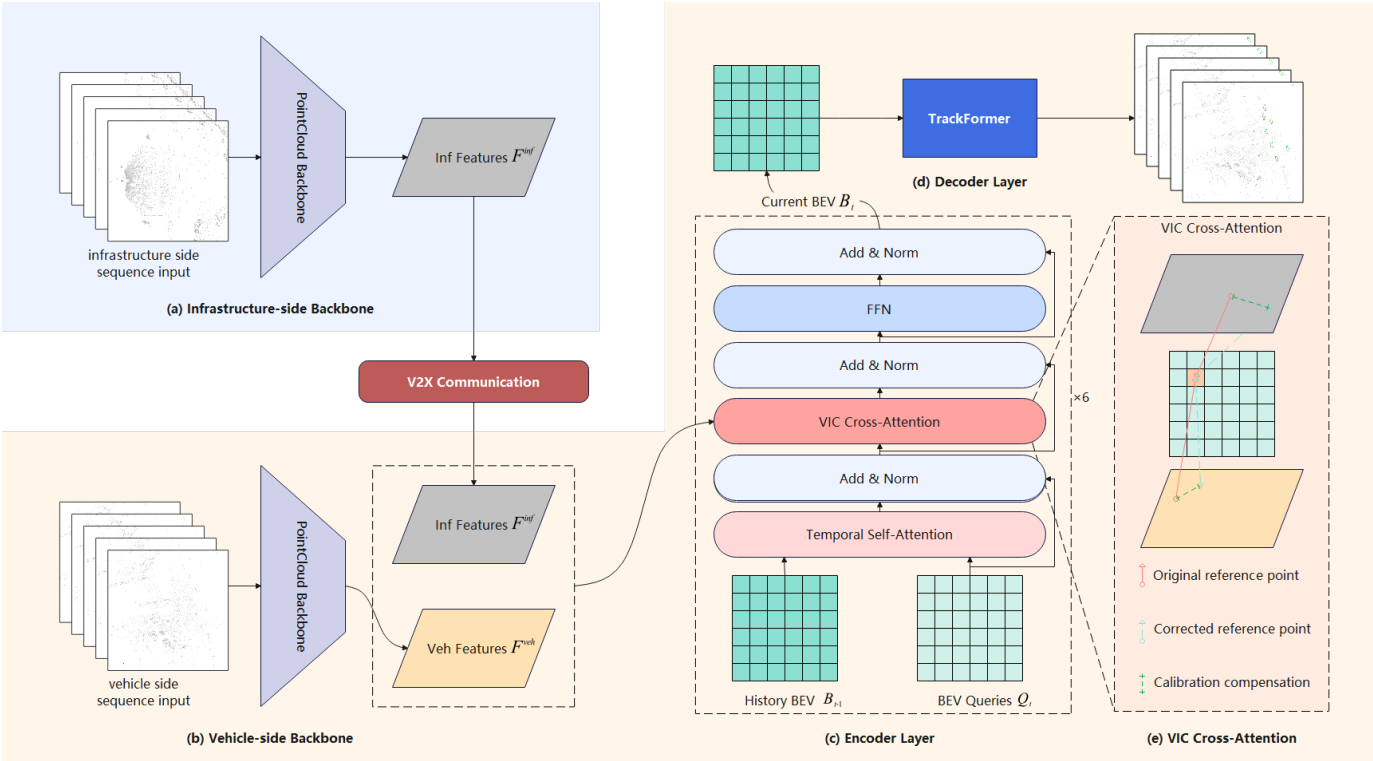

Fig. 3. **Architecture of LET-VIC.** The diagram illustrates the steps involved in the LET-VIC framework. (a) and (b) Both the infrastructure-side and vehicle-side employ PointPillars to extract LiDAR point cloud features. Then the infrastructure-side features are transmitted to the vehicle side through V2X communication and integrated into the VIC cross-attention module along with the vehicle-side features. (c) The BEV encoder of LET-VIC is inspired by BEVFormer. (d) The decoder layers of LET-VIC employ TrackFormer. (e) The VIC Cross-Attention module fuses the Bird's Eye View (BEV) features from both the infrastructure and vehicle sides, compensating for calibration errors.

LiDAR sensors, facilitating a robust understanding of the spatial and temporal characteristics of the objects.

In the context of VIC Detection, the system is designed to identify various objects within the environment. The detection process relies on sequential point cloud data captured over time, allowing for the recognition of objects based on their spatial features. This includes determining the type of objects present, their spatial locations, dimensions and orientations. The integration of data from both vehicle and infrastructure sensors is crucial, as it provides a comprehensive view of the surroundings, improving detection accuracy and robustness against occlusions or limitations inherent to individual sensors.

For the tracking aspect, VIC Tracking focuses on the continuous monitoring of detected objects as they move through the environment. This involves maintaining a unique tracking ID for each object, which allows the system to consistently identify and follow these objects over time. The tracking process is particularly challenging due to factors such as sensor noise, changes in object appearance, and the dynamic nature of the environment. By leveraging sequential data from both the vehicle and infrastructure sides, the system can achieve more stable and reliable tracking of moving objects, even in complex scenarios.

The input of LET-VIC consists of two components:

- Vehicle sequential point clouds $PC_v(t_v^{'})|t_v^{'} \leq t_v$ and their calibration matrix $M_v(t_v^{'})|t_v^{'} \leq t_v$, captured at and prior to time t_v. Here, $PC_v(\cdot)$ denotes the vehicle-side sensor capturing function.
- Infrastructure sequential point clouds $PC_i(t_i^{'})|t_i^{'} \leq t_i$ and their calibration matrix $M_i(t_i^{'})|t_i^{'} \leq t_i$, captured before or at time t_i. Here, $PC_i(\cdot)$ denotes the infrastructure-side sensor capturing function. Note that t_i is earlier than t_v ($t_i < t_v$) due to communication delays.

The outputs of VIC Temporal Perception include the category, location, dimension, orientation, and unique tracking ID of each object in the region of interest surrounding the ego vehicle at time t_v. The corresponding ground truth consists of the set of tracked objects detected and tracked by any of the cooperative-view sensors at time t_v, which can be formulated as:

$$GT = (GT_v \cup GT_i) \cap ROI_{veh}, \tag{1}$$

where GT_v is the ground truth from the vehicle side sensors, GT_i is the ground truth from the infrastructure side sensors, and ROI_{veh} is the ego-vehicle region of interest.

B. BEV Feature Generation

Fig. 4 illustrates how the PointPillars framework [38] is employed on both vehicle and infrastructure sides to process LiDAR point clouds. The raw point cloud data is first organized into pillars—grids that aggregate spatial information—enabling efficient feature extraction for subsequent processing.

The pipeline for BEV feature generation begins by preprocessing the 3D point clouds (x, y, z). In the voxelization step, the point clouds are discretized into 3D grid cells (voxels), with distinct regions of interest (ROI) for vehicle and infrastructure sides. The vehicle side ROI spans x: [-51.2, 51.2] meters, y: [-51.2, 51.2] meters, and z: [-5.0, 3.0] meters, while the infrastructure side ROI covers x: [0, 102.4] meters, y: [-51.2, 51.2] meters, and z: [-5.0, 3.0] meters.

Voxelization uses a uniform voxel size of 0.2 meters along the x and y axes, and 8 meters along the z-axis. As a result, the vehicle-side grid is 512×512, and the infrastructure-side grid is also 512×512. Each voxel stores its corresponding points and their coordinates.

Following voxelization, PillarFeatureNet extracts high-dimensional features from the voxels, transforming the point cloud into a 2D BEV representation. These pseudo-image features are scattered using the PointPillarsScatter layer and are further refined by SECOND convolutional layers. Finally, a Feature Pyramid Network (FPN) integrates multi-scale features, outputting a set of multi-level features to enhance object perception capabilities across different spatial resolutions.

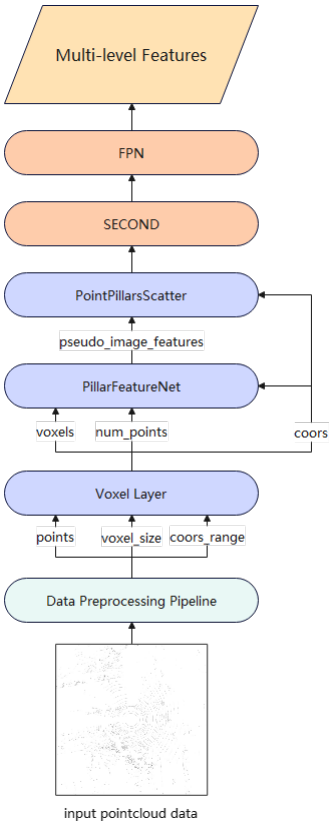

Fig. 4. **PointCloud Backbone.** The PointCloud Backbone extract Bird's Eye View (BEV) features from point cloud data. The pipeline starts with data preprocessing, voxelization, and feature extraction via PillarFeatureNet. Pseudo-image features are then processed by SECOND and FPN, producing multi-level features for object perception at various scales.

C. BEV Feature Transmission

In V2X communication, three primary data types are transmitted: raw data, instance-level perception data, and feature-level intermediate data. Each type incurs different transmission costs and offers varying levels of information retention.

- Raw data includes unprocessed sensor information, like LiDAR point clouds or images. It has the highest transmission cost due to its large volume but retains the most information as it is unfiltered and uncompressed.
- Instance-level perception data consists of processed outputs like detected objects and attributes or queries that contain perception results but are not yet decoded [39]. It has the lowest transmission cost due to high compression, but this also leads to the highest information loss because it transmits only selected information.
- Feature-level intermediate data comprises key features extracted from raw data, such as BEV features [40]. It balances transmission costs and information retention.

Our V2X communication framework prioritizes transmitting BEV features due to the trade-off between transmission cost and information retention. BEV features capture essential spatial relationships and environmental context with reduced data volume, ensuring critical information for accurate perception and decision-making is retained. This approach significantly reduces the required communication bandwidth compared to raw data transmission. Additionally, the VIC Cross-Attention mechanism effectively integrates BEV features from both vehicle and infrastructure sides.

D. BEV Feature Fusion

The deformable attention mechanism plays a critical role in LET-VIC's ability to dynamically fuse features from multiple viewpoints. Traditional attention mechanisms can struggle with multi-view fusion due to high computational costs and difficulties in aligning spatial features across different perspectives. In contrast, deformable attention significantly reduces computational overhead by focusing on a sparse set of key features, known as reference points, and dynamically adjusting its focus based on local feature distributions.

In LET-VIC, the VIC Cross-Attention Module employs deformable attention to integrate BEV features from both vehicle-side and infrastructure-side sensors. The process begins by projecting BEV queries to each perspective and generating initial reference points. A learnable network then predicts calibration adjustments to refine these reference points, compensating for any misalignments between the two perspectives. Deformable attention is subsequently applied around the refined points, enabling the model to sample key features efficiently. This approach ensures that only the most relevant features from both viewpoints are fused, enhancing the efficiency and accuracy of feature integration while accounting for sensor misalignments.

The ability to adaptively focus on critical features enables the deformable attention mechanism to excel in complex, multi-view tracking tasks where spatial alignment may vary due to sensor calibration errors. Fig. 5 illustrates the VIC Cross-Attention mechanism, showcasing its ability to dynamically integrate data across different sensors. The process of VIC Cross-Attention (VICCrossAttn) can be formulated as

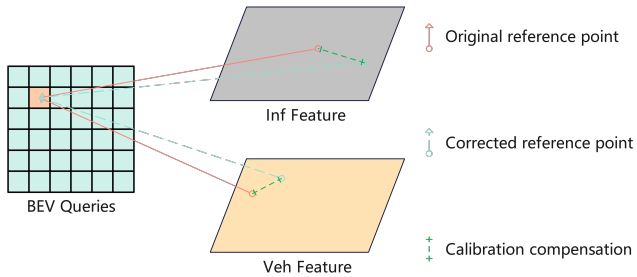

Fig. 5. **VIC Cross-Attention.** The VIC Cross-Attention module fuses the Bird's Eye View (BEV) features from both the infrastructure and vehicle sides, compensating for calibration errors. First, We project BEV queries to both the infrastructure side and vehicle side features to get the original reference point. Then, we use a learnable network to predict the calibration compensation to refine the original reference point. Finally, we use deformable attention sampling around the corrected reference point to generate the respective BEV feature.

follows:

$$\begin{aligned}&\text{VICCrossAttn}(Q^{bev}, F^{veh}, F^{inf}, P^{veh}, P^{inf}) = \\ &\sum_{i=1}^{N_{ref}} \Bigg[\frac{1}{1+\mathcal{M}_i^{inf}} \big(\text{MSDeformAttn}(Q_i^{bev}, P_i^{veh}, F^{veh}) \\ &+ \mathcal{M}_i^{inf} \cdot \text{MSDeformAttn}(Q_i^{bev}, P_i^{inf}, F^{inf})\big)\Bigg], \end{aligned} \tag{2}$$

where i indexes the reference points, and N_{ref} is the total reference points for BEV Query Q^{bev}. $P_i^{veh} \in [0,1]^2$ are the normalized coordinates of the i-th reference points on the vehicle side. $P_i^{inf} \in [0,1]^2$ are the normalized coordinates of the i-th reference points on the infrastructure side. $\mathcal{M}^{inf}$ is the mask matrix ensuring that any reference point projected onto the infrastructure side multi-level LiDAR BEV feature is excluded if it falls outside the feature's bounds.

The multi-scale deformable attention (MSDeformAttn) function is defined as:

$$\begin{aligned}&\text{MSDeformAttn}(Q_i, P_i, \{F^l\}_{l=1}^L) \\ &= \sum_{m=1}^{M} W_m \left[\sum_{l=1}^{L} \sum_{k=1}^{K} A_{mlqk} \cdot W'_m F_i^l(\mathcal{R}_l(P_i) + \Delta p_{mlqk}) \right], \end{aligned} \tag{3}$$

Where $i \in \Omega_i$ indexes a query element with representation feature $Q_i \in \mathbb{R}^C$, where C is the feature dimension. m indexes the attention head, l indexes the input feature level, and k indexes the sampling point. Δp_{mlqk} represents the sampling offset, and A_{mlqk} denotes the attention weight of the k-th sampling point in the l-th feature level and the m-th attention head. The scalar attention weight A_{mlqk} is normalized by $\sum_{l=1}^{L}\sum_{k=1}^{K} A_{mlqk} = 1$. $P_i \in [0,1]^2$ are the normalized coordinates for clarity in scale formulation. The function $\mathcal{R}_l(P_i)$ re-scales the normalized coordinates P_i to the input feature map of the l-th level. $\Delta pmlqk \in \mathbb{R}^2$ are 2-dimensional real numbers with an unconstrained range. $W'_m \in \mathbb{R}^{C/M \times C}$ and $W_m \in \mathbb{R}^{C \times C/M}$ are learnable weights for the m-th attention head.

E. Calibration Error Compensation

Calibration errors in sensors, arising from precision variations, environmental factors, and calibration method uncertainties, pose significant challenges to perception accuracy in autonomous driving systems. Compensating for sensor calibration errors is crucial for LET-VIC as it ensures accurate data fusion and reliable cooperative perception performance. Therefore, we implemented CEC module to optimize spatial error correction during coordinate transformation, delivering precise and robust temporal perception.

Initially, the positions of vehicle-side or infrastructure-side features corresponding to each point in the BEV features are determined through coordinate system transformation. Subsequently, CEC employs a set of learnable parameters that adapt during training to learn adaptive offsets, which include Δx^{inf}, Δy^{inf}, Δx^{veh}, and Δy^{veh}. Finally, the positions of vehicle-side or roadside features corresponding to each BEV feature are adjusted by adding this set of offsets, forming compensated reference points as shown in Eqs. 4 and 5. Then, we normalize the original reference point coordinates according to the specified point cloud range, as detailed in Eqs. 6 and 7.

$$\begin{bmatrix} x_i^{veh} \\ y_i^{veh} \end{bmatrix} = R_{bev2veh} \cdot Ref_i^{bev} + T_{bev2veh} + \begin{bmatrix} \Delta x_i^{veh} \\ \Delta y_i^{veh} \end{bmatrix}, \tag{4}$$

$$\begin{bmatrix} x_i^{inf} \\ y_i^{inf} \end{bmatrix} = R_{bev2inf} \cdot Ref_i^{bev} + T_{bev2inf} + \begin{bmatrix} \Delta x_i^{inf} \\ \Delta y_i^{inf} \end{bmatrix}, \tag{5}$$

$$P_i^{veh} = \begin{bmatrix} \dfrac{x_i^{veh} - x_{min}^{veh}}{x_{max}^{veh} - x_{min}^{veh}} & \dfrac{y_i^{veh} - y_{min}^{veh}}{y_{max}^{veh} - y_{min}^{veh}} \end{bmatrix}, \tag{6}$$

$$P_i^{inf} = \begin{bmatrix} \dfrac{x_i^{inf} - x_{min}^{inf}}{x_{max}^{inf} - x_{min}^{inf}} & \dfrac{y_i^{inf} - y_{min}^{inf}}{y_{max}^{inf} - y_{min}^{inf}} \end{bmatrix}, \tag{7}$$

Where x_i^{veh}, y_i^{veh} represents the i-th original coordinates of the reference point on the vehicle-side and x_i^{inf}, y_i^{inf} represents the i-th original coordinates of the reference point on the infrastructure-side. $R_{bev2inf}$ represents the rotation matrix from the vehicle side LiDAR coordinate system to the pseudo-image coordinate system of infrastructure-side point cloud BEV features, and $T_{bev2inf}$ represents the translation matrix from the vehicle side LiDAR coordinate system to the pseudo-image coordinate system of infrastructure-side point cloud BEV features. Δx_i^{inf} and Δy_i^{inf} represent the calibration errors corresponding to the infrastructure side at i-th reference point; Ref_i^{veh} represents the i-th reference points on the pseudo-image of vehicle side point cloud BEV features, $R_{bev2veh}$ represents the rotation matrix from the vehicle side LiDAR coordinate system to the pseudo-image coordinate system of vehicle side point cloud BEV features, and $T_{bev2veh}$ represents the translation matrix from the vehicle side LiDAR coordinate system to the pseudo-image coordinate system of vehicle side point cloud BEV features; Δx_i^{veh} and Δy_i^{veh} represent the calibration errors corresponding to the vehicle side at i-th reference point. $x_{min}^{v}eh$, $x_{max}^{v}eh$ are the minimum and maximum values of the vehicle side point cloud range in the x-direction, $y_{min}^{v}eh$, $y_{max}^{v}eh$ are the minimum and maximum values of the vehicle side point cloud range in the y-direction. $x_{min}^{i}nf$, $x_{max}^{i}nf$ are the minimum and maximum values of the infrastructure side point cloud range in the x-direction, $y_{min}^{i}nf$, $y_{max}^{i}nf$ are the minimum and maximum

values of the infrastructure side point cloud range in the y-direction. P_i^{veh}, P_i^{inf} are the input parameters defined in Eq. 2.

F. End-to-End Tracking

The end-to-end tracking capability of LET-VIC is powered by an advanced architecture inspired by the TrackFormer framework [5], [6], [34], which unifies object detection and tracking tasks within a single Transformer-based pipeline. This integration bypasses the conventional two-step tracking-by-detection approach, where detection is followed by post-processing for tracking. Instead, LET-VIC directly associates objects across frames during detection, allowing for joint optimization of both tasks.

Within LET-VIC, detect queries and track queries play distinct but complementary roles in the TrackFormer decoder. Detect queries are responsible for identifying new objects in each frame by interacting with the current frame's features, focusing on objects not previously tracked. Track queries, on the other hand, are used to maintain object identities across frames, carrying information from previous frames to ensure temporal consistency by associating the same object across consecutive frames. This combination allows for simultaneous detection and tracking, ensuring seamless object tracking throughout sequences.

LET-VIC's end-to-end design benefits from a joint loss function that simultaneously optimizes detection and tracking. The loss function includes components for object classification, bounding box regression, and identity preservation. This comprehensive approach enhances overall accuracy and ensures that objects are correctly identified and tracked even in complex and dynamic environments.

G. Evaluation Metrics and Analysis

To evaluate LET-VIC's performance, we selected a range of metrics that comprehensively assess both detection and tracking accuracy [41]–[43]. These metrics are standard in 3D tracking benchmarks and provide a balanced view of system performance under various conditions:

- **mAP (Mean Average Precision):** mAP is a key metric for evaluating object detection performance. It measures how accurately detected objects match ground-truth objects across different recall levels, typically using distance thresholds. For each distance threshold, precision-recall curves are generated, and the area under each curve gives the Average Precision (AP). The final mAP score is the mean of AP values across all classes and distance thresholds. A higher mAP indicates better detection quality. The formulations for AP and mAP are:

$$\text{AP} = \int_0^1 \text{precision}(r)dr, \tag{8}$$

$$\text{mAP} = \frac{1}{N}\sum_{c=1}^{N} \text{AP}_c, \tag{9}$$

Where r represents recall levels from 0 to 1, N is the number of classes, and AP_c is the average precision for class c. In practice, the area under the PR curve is often approximated by taking the precision at discrete recall levels.

- **AMOTA (Average Multi-Object Tracking Accuracy):** AMOTA is a central metric for evaluating tracking accuracy in multi-object scenarios. It builds on Multi-Object Tracking Accuracy (MOTA), which assesses tracking accuracy by accounting for false positives, false negatives, and identity switches between tracked objects and ground truth. AMOTA averages MOTA scores across different difficulty levels and recall thresholds, providing an overall measure of tracking accuraciy. Higher AMOTA values are preferred, as they reflect consistent tracking accuracy across recall levels. The formulations for MOTA and AMOTA are:

$$\text{MOTA} = 1 - \frac{\sum_t(\text{FP}_t + \text{FN}_t + \text{IDS}_t)}{\sum_t(\text{GT}_t)}, \tag{10}$$

$$\text{AMOTA} = \frac{1}{R}\sum_{r=1}^{R} \text{MOTA}_r, \tag{11}$$

Where FP_t is the number of false positives at time t, FN_t is the number of false negatives at time t, IDS_t is the number of ID switches at time t, GT_t is the total number of groundtruth objects at time t, R is the number of recall levels, and MOTA_r is the MOTA score at recall level r.

- **AMOTP (Average Multi-Object Tracking Precision):** AMOTP is an essential metric for evaluating tracking precision in multi-object scenarios. It builds on Multi-Object Tracking Precision (MOTP), which measures the spatial alignment between tracked and ground-truth object positions by calculating the average positional error. AMOTP averages MOTP scores across different difficulty levels and recall thresholds, providing an overall measure of tracking precision. Lower AMOTP values are preferred, as they reflect consistent tracking precision across recall levels. The formulations for MOTP and AMOTP are:

$$\text{MOTP} = \frac{\sum_{i,t} d_{i,t}}{\sum_t(c_t)}, \tag{12}$$

$$\text{AMOTP} = \frac{1}{R}\sum_{r=1}^{R} \text{MOTP}_r, \tag{13}$$

Where $d_{i,t}$ is the positional error for the i-th matched object at time t, c_t is the number of successfully matched object pairs at time t, R is the number of recall levels, and MOTP_r is the MOTP score at recall level r.

These metrics offer a thorough evaluation of LET-VIC's detection and tracking performance under varied conditions. We select mAP as our primary detection metric because it effectively measures the accuracy of object identification, providing insight into the model's ability to detect objects with precision. For tracking, we emphasize AMOTA and AMOTP as they capture tracking accuracy and spatial precision across multiple recall thresholds. These metrics provide a comprehensive assessment of LET-VIC's robustness and consistency,

TABLE I
PERFORMANCE COMPARISON UNDER DIFFERENT DELAY CONDITIONS ON THE V2X-SEQ-SPD 10HZ DATASET V2VNET, FFNET, AND POINTPILLARS FOLLOWS THE TRACKING-BY-DETECTION PARADIGM WITH MULTI-VIEW POINT CLOUD FEATURE FUSION, LET-V IS AN END-TO-END TRACKING MODEL WITH SINGLE-VIEW POINT CLOUD DATA INPUT, LET-VIC IS AN END-TO-END TRACKING MODEL THAT FUSES MULTI-VIEW POINT CLOUD DATA FEATURE. DETECTION USES MAP AND TRACKING USES AMOTA AND AMOTP.

Model	Latency 0ms			Latency 100ms			Latency 200ms			Latency 300ms		
	mAP↑	AMOTA↑	AMOTP↓	mAP↑	AMOTA↑	AMOTP↓	mAP↑	AMOTA↑	AMOTP↓	mAP↑	AMOTA↑	AMOTP↓
LET-V (Ours)	0.456	0.467	1.113	-	-	-	-	-	-	-	-	-
V2VNet [18]	0.349	0.377	1.258	0.346	0.386	1.268	0.341	0.386	1.268	0.333	0.362	1.309
FFNet [22]	0.349	0.377	1.258	0.340	0.377	1.261	0.345	0.383	1.262	0.342	0.387	1.264
PointPillars [38]	0.469	0.509	0.822	0.456	0.510	0.833	0.444	0.486	0.875	0.441	0.478	0.874
LET-VIC (Ours)	**0.606**	**0.640**	**0.700**	**0.579**	**0.631**	**0.716**	**0.554**	**0.613**	**0.775**	**0.526**	**0.570**	**0.811**

especially in complex, real-world environments where accurate object identification and stable tracking are critical.

IV. EXPERIMENTS

In this section, we evaluate the performance of LET-VIC on V2X-Seq-SPD dataset [9]. For better comparison, we also develop and reproduce four methods, including one single-view end-to-end method: LET-V, and three multi-view tracking-by-detection methods: V2VNet [18], FFNet [22], and PointPillars [38] with tracking method AB3DMOT [43]. The experimental results indicate that our method can significantly improve performance over the compared methods.

A. Experiment Settings

1) Dataset: We use the V2X-Seq-SPD dataset [9], which contains complex traffic intersection scenes captured at 10Hz using both vehicle-side and infrastructure-side sensors. The dataset provides detailed 3D tracking annotations for multiple object classes, such as cars, pedestrians, and cyclists. The dataset is split into *train/validation/test* (5:2:3).

2) LET-VIC Implementation Details: We extract V2X-Seq-SPD [9] at a frequency of 10Hz to create the V2X-Seq-SPD-10Hz dataset, aligning with nuScenes [41]. The ego vehicle-side BEV range configuration is $[-51.2, 51.2, -51.2, 51.2]$ meters with grids sized at 0.512 meters $\times$ 0.512 meters. Considering the infrastructure-side LiDAR's fan-shaped perception, the infrastructure-side BEV range configuration is $[0, 102.4, -51.2, 51.2]$ meters with grids sized at 0.512 meters $\times$ 0.512 meters. Our evaluation encompasses all tasks utilizing cooperative-view annotations, and the experiments are conducted using the NVIDIA A100 GPU.

3) Baseline Settings: We select single-vehicle temporal perception and non-end-to-end VIC perception as two baselines, comparing our approach against state-of-the-art (SOTA) LiDAR-based VIC perception methods, including V2VNet, FFNet, and PointPillars.

- **LET-V:** Using only ego-vehicle point cloud data as input, LET-V is trained within the LET-VIC framework without incorporating infrastructure data. The model is end-to-end and directly outputs detection and tracking results during inference.
- **V2VNet:** Detection is performed using V2VNet [18], paired with AB3DMOT [43] for tracking in a tracking-by-detection framework. The model is trained on fused features from both ego-vehicle and infrastructure point clouds. Evaluation includes delay scenarios of 0 ms, 100 ms, 200 ms, and 300 ms.
- **FFNet:** Detection is performed using FFNet [22], paired with AB3DMOT [43] for tracking in a tracking-by-detection framework. The model is trained on fused features from both ego-vehicle and infrastructure point

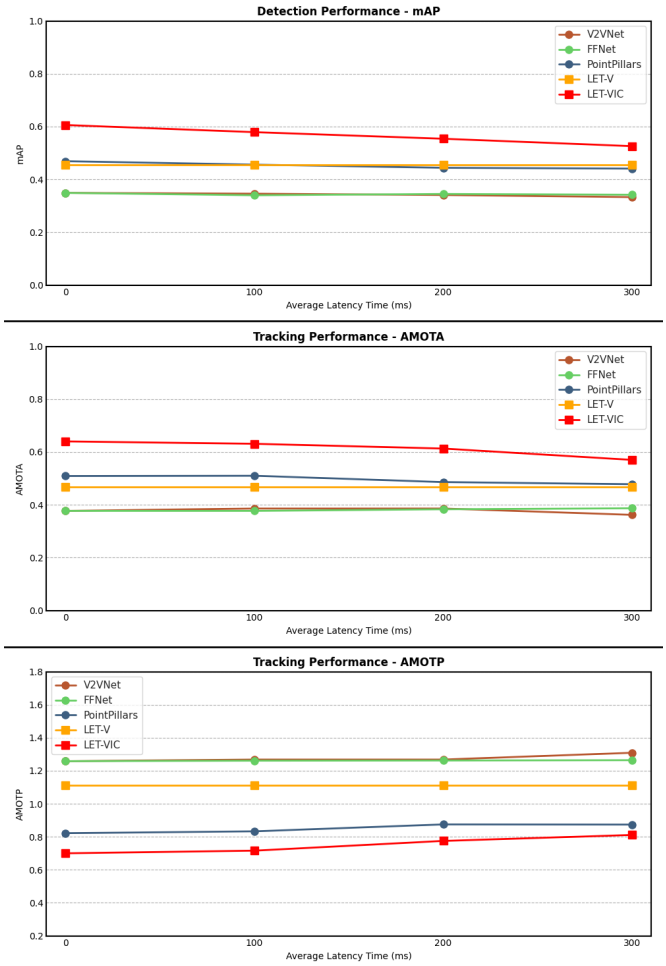

Fig. 6. **Performance Comparison under Different Latency Conditions.** Our proposed LET-VIC model significantly enhances perception performance through multi-perspective fusion in Vehicle-Infrastructure Cooperation (VIC), achieving the best performance across all metrics and under all latency conditions compared to all baseline models.

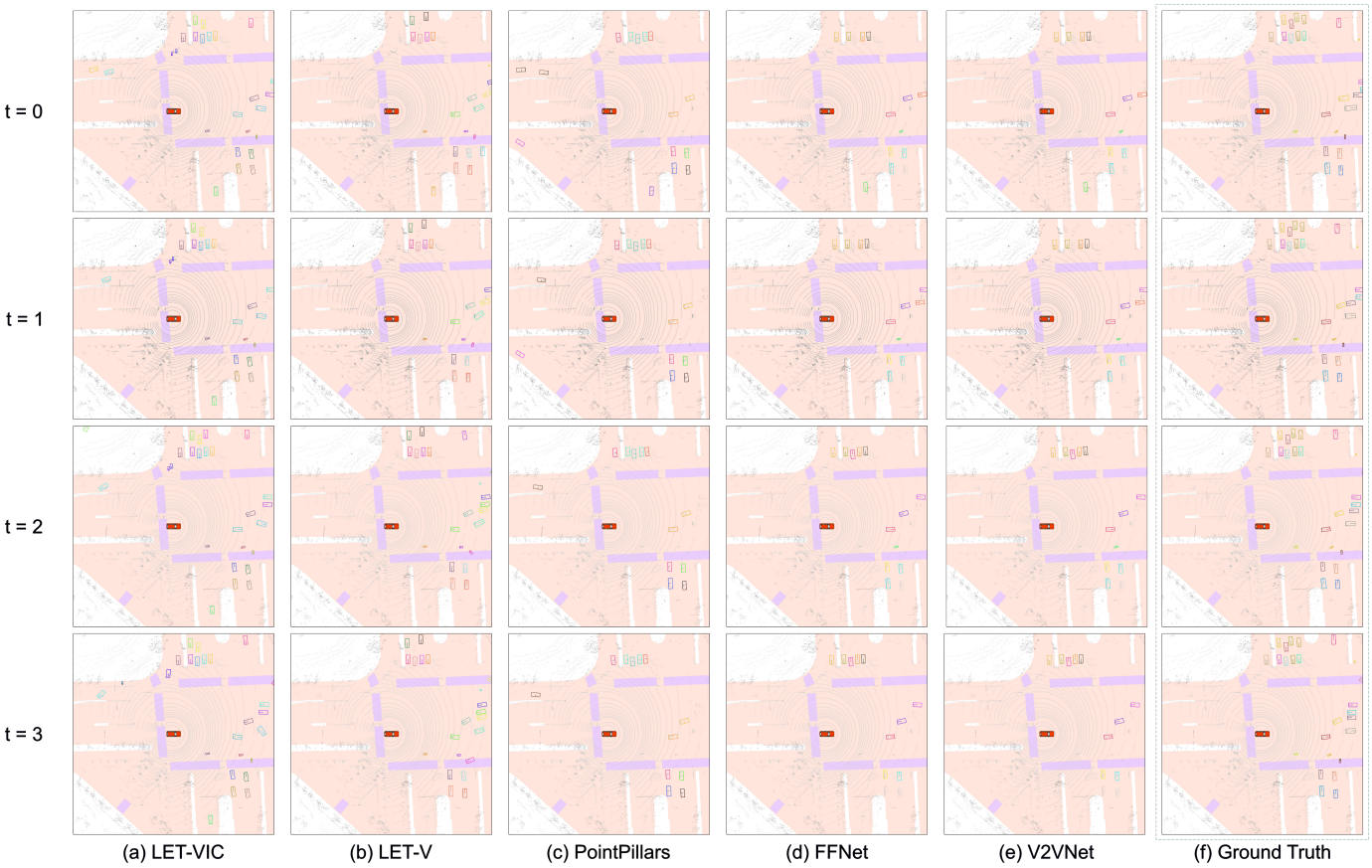

Fig. 7. **Visualization with V2X-Seq-SPD.** The visualization comparison clearly demonstrates that our LET-VIC model achieves superior results compared to other baseline models. Each row represents the perception results of each model at time t. Each column shows the temporal perception results of a specific model, with the same color box used for each tracked object. Panel (a) shows the temporal perception results of LET-VIC, (b) represents LET-V, (c) shows PointPillars, (d) shows FFNet, (e) shows V2VNet, and (f) represents ground truth.

clouds. Evaluation includes delay scenarios of 0 ms, 100 ms, 200 ms, and 300 ms.

- **PointPillars:** Detection is performed using PointPillars [38], paired with AB3DMOT [43] for tracking in a tracking-by-detection framework. The model is trained on fused features from both ego-vehicle and infrastructure point clouds. Evaluation includes delay scenarios of 0 ms, 100 ms, 200 ms, and 300 ms.

B. Experiment Results

Table I and Fig. 6 report the comparative detection and tracking performance of different methods on the V2X-Seq-SPD 10Hz Dataset [9], and LET-VIC shows superior performance on all metrics. Visualizations of each model's inference results are shown in the fig. 7. The comparison of LET-VIC and LET-V, both in the benchmark results and visualizations, demonstrates the advantage of VIC over single-vehicle perception, underscoring the value of incorporating infrastructure-side information. Furthermore, the evaluation and visual results of LET-VIC, PointPillars, FFNet, and V2VNet highlight the benefits of end-to-end temporal perception, showing that integrating historical temporal information significantly enhances perception performance.

1) Comparative Results of VIC Perception and Single-Vehicle Perception: The comparative results of LET-VIC and LET-V demonstrate that LET-VIC consistently outperforms LET-V under various delay conditions, highlighting its strong robustness to latency. Leveraging the VIC Cross-Attention module, LET-VIC effectively integrates BEV features from infrastructure sensors, significantly enhancing detection accuracy and tracking performance with minimal degradation, even under delayed conditions. Specifically, in detection performance, LET-VIC achieves substantial improvements over LET-V, with **+15.0%** mAP at 0ms, **+12.3%** mAP at 100ms, **+9.8%** mAP at 200ms and **+7.0%** mAP at 300ms. For tracking performance, LET-VIC outperforms LET-V with **+17.3%** AMOTA at 0 ms, **+16.4%** AMOTA at 100 ms, **+14.6%** AMOTA at 200 ms and **+10.3%** AMOTA at 300 ms. Moreover, LET-VIC consistently achieves lower AMOTP values than LET-V, with **-0.413** AMOTP at 0 ms, **-0.397** AMOTP at 100 ms, **-0.338** AMOTP at 200 ms and **-0.302** AMOTP at 300 ms, reflecting superior localization accuracy. Additionally, as shown in Fig. 6, although each metric shows a slight decline within a latency range up to 300 ms, LET-VIC still surpasses LET-V by **+7.0%** in mAP, **+10.3%** in AMOTA, and **-0.302** in AMOTP at 300 ms delay, demonstrating its ability to effectively fuse infrastructure features under certain delays and enhance perception capabilities, showcasing robustness to latency.

TABLE II
IMPORTANCE OF CEC IN LET-VIC ON THE V2X-SEQ-SPD 2HZ DATASET AT DIFFERENT LATENCY LEVELS.

CEC	Latency (ms)	mAP ↑	AMOTA ↑	AMOTP ↓
	0	0.198	0.092	1.653
✓		**0.262**	**0.139**	**1.615**
	100	0.206	0.120	1.647
✓		**0.281**	**0.175**	**1.568**
	200	0.204	0.118	1.652
✓		**0.254**	**0.136**	**1.608**
	300	0.191	0.099	1.653
✓		**0.243**	**0.141**	**1.611**

2) Comparative Results of End-to-End Paradigms and Tracking-by-Detection Paradigms: The comparative results between LET-VIC and models such as V2VNet [18], FFNet [22], and PointPillars [38] indicate that the end-to-end temporal perception approach of LET-VIC significantly outperforms traditional tracking-by-detection models across various delay settings. Specifically, LET-VIC achieves substantial improvements in detection performance, with at least **+13.7%** mAP at 0ms, **+12.3%** mAP at 100ms, **+11.0%** mAP at 200ms and **+8.5%** mAP at 300ms compared to the other models. For tracking performance, LET-VIC outperforms V2VNet, FFNet, and PointPillars with at least **+13.1%** AMOTA at 0 ms, **+12.1%** AMOTA at 100 ms, **+12.7%** AMOTA at 200 ms and **+9.2%** AMOTA at 300 ms. Moreover, LET-VIC consistently achieves lower AMOTP values, with at least **-0.122** AMOTP at 0 ms, **-0.117** AMOTP at 100 ms, **-0.100** AMOTP at 200 ms and **-0.063** AMOTP at 300 ms, reflecting superior localization accuracy. Additionally, Compared to V2VNet, FFNet, and PointPillars, LET-V demonstrates that even with single-vehicle perception, the end-to-end approach significantly improves detection and tracking. Its performance approaches that of PointPillars and surpasses both FFNet and V2VNet. This highlights the effectiveness of the end-to-end paradigm in enhancing perception performance, even without infrastructure data.

C. Ablation Study

This section investigates the impact of our CEC module on perception accuracy. Calibration errors can significantly degrade tracking performance, and our module is designed to mitigate these effects.

1) Experimental Setup: We compare the performance of the LET-VIC model with and without the CEC module under delays of 0 ms, 100 ms, 200 ms, and 300 ms. The dataset annotations are used without manual error compensation to highlight the module's effectiveness.

2) LET-VIC Implementation Details: Due to limited computational resources, this section of experiments extracts the V2X-Seq-SPD dataset at a reduced frequency of 2Hz to generate the V2X-Seq-SPD-2Hz dataset. Additionally, we reduced the feature dimensionality in the model from 256 dimensions to 64 dimensions to expedite training and evaluation. Other settings remain consistent with those described in Section IV-A2.

3) Analysis: The results presented in Table II demonstrate that LET-VIC with the CEC module consistently outperforms the standard LET-VIC across all delay settings, highlighting the CEC module's effectiveness in enhancing perception robustness. Specifically, LET-VIC with calibration error compensation achieves **+6.4%** mAP and **+4.7%** AMOTA improvements, along with a **-0.038** AMOTP reduction at 0 ms delay; **+7.5%** mAP, **+5.5%** AMOTA, and **-0.079** AMOTP at 100 ms delay; **+5.0%** mAP, **+1.8%** AMOTA, and **-0.044** AMOTP at 200 ms delay; and **+5.2%** mAP, **+4.2%** AMOTA, and **-0.042** AMOTP at 300 ms delay. By compensating for sensor calibration errors, this module improves multi-view feature fusion, leading to better overall performance and demonstrating LET-VIC's robustness to calibration inaccuracies.

V. CONCLUSION

This paper introduces LET-VIC, a LiDAR-based end-to-end tracking framework for VIC. By integrating information from multi-view sensor sources, LET-VIC addresses the limitations of single-view perception and enhances the system's ability to detect and track objects. Through its end-to-end design, LET-VIC effectively incorporates temporal information to maintain object identity across frames in both detection and tracking, significantly improving performance in dynamic environments. Moreover, its feature fusion approach compensates for spatial calibration errors during vehicle-infrastructure coordinate transformations, ensuring robust and accurate object perception. Experimental results on the V2X-Seq-SPD dataset confirm the effectiveness of this approach, demonstrating substantial improvements in tracking performance and system robustness.

a) Limitations and Future Work: LET-VIC, while effective, is limited by relying solely on point cloud inputs from LiDAR sensors. Although point clouds provide accurate depth and 3D structure, they lack color and texture details, affecting the recognition of fine object attributes. Additionally, point clouds can become sparse at longer distances or in complex environments, impacting detection and tracking accuracy. Conversely, image data offers rich semantic information but lacks depth. Future work will focus on fusing point cloud and image features to enhance both spatial perception and semantic understanding, improving overall system performance in complex environments. Another limitation is the lack of compensation for communication delays in VIC, which can affect real-time tracking performance. Future research will address this by developing strategies to mitigate temporal delays, ensuring more accurate and robust tracking across multi-view sensors.

REFERENCES

[1] S. Chen, J. Hu, Y. Shi, Y. Peng, J. Fang, R. Zhao, and L. Zhao, "Vehicle-to-everything (v2x) services supported by lte-based systems and 5g," *IEEE Communications Standards Magazine*, vol. 1, no. 2, pp. 70–76, 2017.

[2] S. Gyawali, S. Xu, Y. Qian, and R. Q. Hu, "Challenges and solutions for cellular based v2x communications," *IEEE Communications Surveys & Tutorials*, vol. 23, no. 1, pp. 222–255, 2020.

[3] S. Maaloul, H. Aniss, M. Kassab, and M. Berbineau, "Classification of c-its services in vehicular environments," *IEEE Access*, vol. 9, pp. 117 868–117 879, 2021.

[4] C. Zhang, C. Zhang, Y. Guo, L. Chen, and M. Happold, "Motiontrack: end-to-end transformer-based multi-object tracking with lidar-camera fusion," in *Proceedings of the IEEE/CVF Conference on Computer Vision and Pattern Recognition*, 2023, pp. 151–160.

[5] T. Meinhardt, A. Kirillov, L. Leal-Taixe, and C. Feichtenhofer, "Trackformer: Multi-object tracking with transformers," in *Proceedings of the IEEE/CVF conference on computer vision and pattern recognition*, 2022, pp. 8844–8854.

[6] F. Zeng, B. Dong, Y. Zhang, T. Wang, X. Zhang, and Y. Wei, "Motr: End-to-end multiple-object tracking with transformer," in *European Conference on Computer Vision*. Springer, 2022, pp. 659–675.

[7] X. Zhou, V. Koltun, and P. Krähenbühl, "Tracking objects as points," in *European conference on computer vision*. Springer, 2020, pp. 474–490.

[8] T. Yin, X. Zhou, and P. Krahenbuhl, "Center-based 3d object detection and tracking," in *Proceedings of the IEEE/CVF conference on computer vision and pattern recognition*, 2021, pp. 11 784–11 793.

[9] H. Yu, W. Yang, H. Ruan, Z. Yang, Y. Tang, X. Gao, X. Hao, Y. Shi, Y. Pan, N. Sun *et al.*, "V2x-seq: A large-scale sequential dataset for vehicle-infrastructure cooperative perception and forecasting," in *Proceedings of the IEEE/CVF Conference on Computer Vision and Pattern Recognition*, 2023, pp. 5486–5495.

[10] K. Sehla, T. M. T. Nguyen, G. Pujolle, and P. B. Velloso, "Resource allocation modes in c-v2x: from lte-v2x to 5g-v2x," *IEEE Internet of Things Journal*, vol. 9, no. 11, pp. 8291–8314, 2022.

[11] X. Cheng, D. Duan, S. Gao, and L. Yang, "Integrated sensing and communications (isac) for vehicular communication networks (vcn)," *IEEE Internet of Things Journal*, vol. 9, no. 23, pp. 23 441–23 451, 2022.

[12] J. Jang, J. Baek, K. Lim, Y. Ro, S. Yoon, and S. Jang, "A study on v2i based cooperative autonomous driving," in *2023 International Conference on Electronics, Information, and Communication (ICEIC)*. IEEE, 2023, pp. 1–3.

[13] S. Lu, F. Liu, Y. Li, K. Zhang, H. Huang, J. Zou, X. Li, Y. Dong, F. Dong, J. Zhu *et al.*, "Integrated sensing and communications: Recent advances and ten open challenges," *IEEE Internet of Things Journal*, 2024.

[14] Q. Chen, S. Tang, Q. Yang, and S. Fu, "Cooper: Cooperative perception for connected autonomous vehicles based on 3d point clouds," in *2019 IEEE 39th International Conference on Distributed Computing Systems (ICDCS)*. IEEE, 2019, pp. 514–524.

[15] Y. Li, S. Ren, P. Wu, S. Chen, C. Feng, and W. Zhang, "Learning distilled collaboration graph for multi-agent perception," *Advances in Neural Information Processing Systems*, vol. 34, pp. 29 541–29 552, 2021.

[16] R. Xu, H. Xiang, X. Xia, X. Han, J. Li, and J. Ma, "Opv2v: An open benchmark dataset and fusion pipeline for perception with vehicle-to-vehicle communication," in *2022 International Conference on Robotics and Automation (ICRA)*. IEEE, 2022, pp. 2583–2589.

[17] Q. Chen, X. Ma, S. Tang, J. Guo, Q. Yang, and S. Fu, "F-cooper: Feature based cooperative perception for autonomous vehicle edge computing system using 3d point clouds," in *Proceedings of the 4th ACM/IEEE Symposium on Edge Computing*, 2019, pp. 88–100.

[18] T.-H. Wang, S. Manivasagam, M. Liang, B. Yang, W. Zeng, and R. Urtasun, "V2vnet: Vehicle-to-vehicle communication for joint perception and prediction," in *Computer Vision–ECCV 2020: 16th European Conference, Glasgow, UK, August 23–28, 2020, Proceedings, Part II 16*. Springer, 2020, pp. 605–621.

[19] J. Cui, H. Qiu, D. Chen, P. Stone, and Y. Zhu, "Coopernaut: End-to-end driving with cooperative perception for networked vehicles," in *Proceedings of the IEEE/CVF Conference on Computer Vision and Pattern Recognition*, 2022, pp. 17 252–17 262.

[20] D. Yang, K. Yang, Y. Wang, J. Liu, Z. Xu, R. Yin, P. Zhai, and L. Zhang, "How2comm: Communication-efficient and collaboration-pragmatic multi-agent perception," in *Thirty-seventh Conference on Neural Information Processing Systems*, 2023.

[21] R. Xu, H. Xiang, Z. Tu, X. Xia, M.-H. Yang, and J. Ma, "V2x-vit: Vehicle-to-everything cooperative perception with vision transformer," in *European conference on computer vision*. Springer, 2022, pp. 107–124.

[22] H. Yu, Y. Tang, E. Xie, J. Mao, P. Luo, and Z. Nie, "Flow-based feature fusion for vehicle-infrastructure cooperative 3d object detection," in *Advances in Neural Information Processing Systems (NeurIPS)*, 2023.

[23] J. Zhong, H. Yu, T. Zhu, J. Xu, W. Yang, Z. Nie, and C. Sun, "Leveraging temporal contexts to enhance vehicle-infrastructure cooperative perception," *arXiv preprint arXiv:2408.10531*, 2024.

[24] H. Ruan, H. Yu, W. Yang, S. Fan, Y. Tang, and Z. Nie, "Learning cooperative trajectory representations for motion forecasting," *arXiv preprint arXiv:2311.00371*, 2023.

[25] J. Philion and S. Fidler, "Lift, splat, shoot: Encoding images from arbitrary camera rigs by implicitly unprojecting to 3d," in *Computer Vision–ECCV 2020: 16th European Conference, Glasgow, UK, August 23–28, 2020, Proceedings, Part XIV 16*. Springer, 2020, pp. 194–210.

[26] J. Huang and G. Huang, "Bevdet4d: Exploit temporal cues in multi-camera 3d object detection," *arXiv preprint arXiv:2203.17054*, 2022.

[27] Y. Li, Z. Ge, G. Yu, J. Yang, Z. Wang, Y. Shi, J. Sun, and Z. Li, "Bevdepth: Acquisition of reliable depth for multi-view 3d object detection," in *Proceedings of the AAAI Conference on Artificial Intelligence*, vol. 37, no. 2, 2023, pp. 1477–1485.

[28] Y. Li, H. Bao, Z. Ge, J. Yang, J. Sun, and Z. Li, "Bevstereo: Enhancing depth estimation in multi-view 3d object detection with temporal stereo," in *Proceedings of the AAAI Conference on Artificial Intelligence*, vol. 37, no. 2, 2023, pp. 1486–1494.

[29] A. W. Harley, Z. Fang, J. Li, R. Ambrus, and K. Fragkiadaki, "Simplebev: What really matters for multi-sensor bev perception?" in *2023 IEEE International Conference on Robotics and Automation (ICRA)*. IEEE, 2023, pp. 2759–2765.

[30] Y. Li, B. Huang, Z. Chen, Y. Cui, F. Liang, M. Shen, F. Liu, E. Xie, L. Sheng, W. Ouyang *et al.*, "Fast-bev: A fast and strong bird's-eye view perception baseline," *IEEE Transactions on Pattern Analysis and Machine Intelligence*, 2024.

[31] H. Zhou, Z. Ge, Z. Li, and X. Zhang, "Matrixvt: Efficient multi-camera to bev transformation for 3d perception," in *Proceedings of the IEEE/CVF International Conference on Computer Vision*, 2023, pp. 8548–8557.

[32] Z. Li, W. Wang, H. Li, E. Xie, C. Sima, T. Lu, Y. Qiao, and J. Dai, "Bevformer: Learning bird's-eye-view representation from multi-camera images via spatiotemporal transformers," in *European conference on computer vision*. Springer, 2022, pp. 1–18.

[33] K. Li, Y. Wang, J. Zhang, P. Gao, G. Song, Y. Liu, H. Li, and Y. Qiao, "Uniformer: Unifying convolution and self-attention for visual recognition," *IEEE Transactions on Pattern Analysis and Machine Intelligence*, vol. 45, no. 10, pp. 12 581–12 600, 2023.

[34] Y. Hu, J. Yang, L. Chen, K. Li, C. Sima, X. Zhu, S. Chai, S. Du, T. Lin, W. Wang *et al.*, "Planning-oriented autonomous driving," in *Proceedings of the IEEE/CVF Conference on Computer Vision and Pattern Recognition*, 2023, pp. 17 853–17 862.

[35] J. Yin, J. Shen, R. Chen, W. Li, R. Yang, P. Frossard, and W. Wang, "Is-fusion: Instance-scene collaborative fusion for multimodal 3d object detection," in *Proceedings of the IEEE/CVF Conference on Computer Vision and Pattern Recognition*, 2024, pp. 14 905–14 915.

[36] Z. Liu, H. Tang, A. Amini, X. Yang, H. Mao, D. L. Rus, and S. Han, "Bevfusion: Multi-task multi-sensor fusion with unified bird's-eye view representation," in *2023 IEEE international conference on robotics and automation (ICRA)*. IEEE, 2023, pp. 2774–2781.

[37] C. Hu, H. Zheng, K. Li, J. Xu, W. Mao, M. Luo, L. Wang, M. Chen, K. Liu, Y. Zhao *et al.*, "Fusionformer: A multi-sensory fusion in bird's-eye-view and temporal consistent transformer for 3d objection," *arXiv preprint arXiv:2309.05257*, 2023.

[38] A. H. Lang, S. Vora, H. Caesar, L. Zhou, J. Yang, and O. Beijbom, "Pointpillars: Fast encoders for object detection from point clouds," in *Proceedings of the IEEE/CVF conference on computer vision and pattern recognition*, 2019, pp. 12 697–12 705.

[39] S. Fan, H. Yu, W. Yang, J. Yuan, and Z. Nie, "Quest: Query stream for vehicle-infrastructure cooperative perception," *arXiv preprint arXiv:2308.01804*, 2023.

[40] Z. Chen, Y. Shi, and J. Jia, "Transiff: An instance-level feature fusion framework for vehicle-infrastructure cooperative 3d detection with transformers," in *Proceedings of the IEEE/CVF International Conference on Computer Vision*, 2023, pp. 18 205–18 214.

[41] H. Caesar, V. Bankiti, A. H. Lang, S. Vora, V. E. Liong, Q. Xu, A. Krishnan, Y. Pan, G. Baldan, and O. Beijbom, "nuscenes: A multimodal dataset for autonomous driving," in *Proceedings of the IEEE/CVF conference on computer vision and pattern recognition*, 2020, pp. 11 621–11 631.

[42] A. Geiger, P. Lenz, C. Stiller, and R. Urtasun, "Vision meets robotics: The kitti dataset," *The International Journal of Robotics Research*, vol. 32, no. 11, pp. 1231–1237, 2013.

[43] X. Weng, J. Wang, D. Held, and K. Kitani, "3d multi-object tracking: A baseline and new evaluation metrics," in *2020 IEEE/RSJ International Conference on Intelligent Robots and Systems (IROS)*. IEEE, 2020, pp. 10 359–10 366.